Self-Heating, Bistability, and Thermal Switching in Organic Semiconductors

A. Fischer,* P. Pahner, B. Lüssem, K. Leo, and R. Scholz
Institut für Angewandte Photophysik, Technische Universität Dresden, George-Bähr-Straße 1, 01069 Dresden, Germany

T. Koprucki,† K. Gärtner, and A. Glitzky
Weierstraß-Institut, Mohrenstraße 39, 10117 Berlin, Germany

(Received 19 September 2012; published 21 March 2013)

We demonstrate electric bistability induced by the positive feedback of self-heating onto the thermally activated conductivity in a two-terminal device based on the organic semiconductor C_{60}. The central undoped layer with a thickness of 300 nm is embedded between thinner *n*-doped layers adjacent to the contacts, minimizing injection barriers. The observed current-voltage characteristics follow the general theory for thermistors described by an Arrhenius-like conductivity law. Our findings include hysteresis phenomena and are of general relevance for the entire material class since most organic semiconductors can be described by a thermally activated conductivity.

DOI: 10.1103/PhysRevLett.110.126601 PACS numbers: 72.20.Pa, 72.80.Rj, 81.05.Fb, 85.80.Fi

The crucial role of Joule heating on the performance of organic electronic devices has been demonstrated for organic light-emitting diodes (OLEDs) [1–3] as well as for fast organic rectifying diodes [4]. An important feature of disordered organic semiconductors is hopping transport, which leads to Arrhenius-like mobility laws and thus to an increase of the conductivity with rising temperature [5–7]. Current flow causes heating of the device; the higher temperature increases the conductivity and thereby creates more current flow, leading to a positive feedback loop. Together with heat losses to the surroundings, this is described by the classical theory of self-heating and thermal runaway.

Self-heating phenomena were first studied in the investigation of the electrical breakdown of dielectrics induced by a thermal runaway [8,9], where above a certain threshold voltage the cooling of the device is no longer sufficient to keep the system in a stationary state. Furthermore, self-heating induces many thermal runaway and switching phenomena, including chemical reactions [10], thermistors [11,12], semiconductors [13,14], and transport through thin films [15–17]. For solid-state electronic devices, it is well-known that due to this electrothermal feedback loop, regions of negative differential resistance (NDR) can appear in the current-voltage characteristics [18]. To our knowledge, NDR phenomena induced by self-heating have not yet been found for organic semiconductor devices.

For materials with Arrhenius-like conductivity laws, NDR phenomena such as thermal switching induced by self-heating only occur for activation energies $E_{\mathrm{act}} > 4k_BT_a$, where k_B denotes Boltzmann's constant and T_a is the ambient temperature; see Ref. [18]. To motivate our expectation of NDR in organic semiconductors, we look at the basic organic mobility model for low fields and low densities given by

$$\mu(T) = \mu_0 \exp\left[-C\left(\frac{\sigma}{k_BT}\right)^2\right],$$

where σ describes the disorder of energy levels and $C \approx 0.4$ [6,7]. The mobility is increasing with the temperature and can be locally approximated by an Arrhenius law with an activation energy $E_{\mathrm{act}} = 2C\sigma^2/(k_BT_a)$. Typical values of the disorder parameter $\sigma = 2$–$6\ k_BT_a$ result in activation energies between about $3k_BT_a$ and $30k_BT_a$. However, the activation energy may be reduced due to a dependence on the carrier density; see Ref. [6] for a detailed discussion. Finally, injection as well as energy barriers between adjacent organic layers in the range of several tenths of an eV should be mentioned as a reason for temperature-activated charge transport [19].

Since activation energies above $4k_BT_a$ are quite common in organic semiconductors, electrothermal bistability or NDR phenomena due to the positive feedback between Joule heating and conductivity have to be expected. Here, we demonstrate this effect for a vertical crossbar structure based on the organic semiconductor C_{60}. Measurements of the current-voltage characteristics reveal an abrupt turnover from a state with low conductivity to a state with high conductivity, in agreement with the predictions by theory.

The direct observation of thermal switching requires a well-defined setup with respect to temperature, thermal resistance, current, Joule heat, and contact and series resistance. We aim on hysteresis loops with large height and width, without damaging the device by thermal runaway. To this end, we summarize the theory of self-heating for a thermally activated conductivity and suppose in the following that the isothermal current-voltage relation for the circuit is given by a power law

$$I_{\mathrm{iso}}(U,T) = I_{\mathrm{ref}}\left(\frac{U}{U_{\mathrm{ref}}}\right)^{\alpha} F(T) \qquad (1)$$

with a positive exponent α and a temperature-dependent conductivity factor $F(T)$ resulting from an Arrhenius law

$$F(T) = \exp\left[-\frac{E_{\rm act}}{k_B}\left(\frac{1}{T}-\frac{1}{T_a}\right)\right]. \quad (2)$$

The quantities $U_{\rm ref}$, $I_{\rm ref}$, and $P_{\rm ref} = U_{\rm ref} I_{\rm ref}$ denote reference values for voltage, current, and power, respectively. The homogeneous steady states of the device are given by equilibria of the global heat balance equation expressing that the dissipated Joule power $\dot{Q}_2 = IU$ equals the heat loss $\dot{Q}_1 = \frac{1}{\Theta_{\rm th}}(T - T_a)$ to the surrounding described by the thermal resistance $\Theta_{\rm th}$,

$$\frac{1}{\Theta_{\rm th}}(T - T_a) = P_{\rm ref}\left(\frac{U}{U_{\rm ref}}\right)^{\alpha+1} F(T). \quad (3)$$

The self-consistent current-voltage characteristic including self-heating parametrized by the temperature $T \geq T_a$ is obtained by combining Eqs. (1) and (3),

$$U(T) = U_{\rm ref}\left(\frac{T - T_a}{\Theta_{\rm th} P_{\rm ref}}\right)^{1/\alpha+1} F(T)^{(-1/\alpha+1)}, \quad (4)$$

$$I(T) = I_{\rm ref}\left(\frac{T - T_a}{\Theta_{\rm th} P_{\rm ref}}\right)^{\alpha/\alpha+1} F(T)^{1/\alpha+1}. \quad (5)$$

Different points on the self-consistent current-voltage characteristic correspond to different values of the temperature rise $T - T_a$. The differential resistance of this S-shaped curve has the form

$$\frac{dU}{dI} = \frac{1 - (T - T_a)\frac{d}{dT}\ln F(T)}{\alpha + (T - T_a)\frac{d}{dT}\ln F(T)}\frac{U}{I}. \quad (6)$$

For $T - [(d/dT)\ln F(T)]^{-1} > T_a$, a region of negative differential resistance is obtained. In the Arrhenius-type temperature dependence of Eq. (2), a NDR region only appears for activation energies $E_{\rm act} > 4k_B T_a$. This can be seen in Fig. 1 where the self-consistent IV curve of such an intrinsic device according to Eqs. (4) and (5) is shown for an isothermal Ohmic current-voltage relation ($\alpha = 1$, $U_{\rm ref}/I_{\rm ref} = 2000\ \Omega$). The turnover points of the S-shaped IV curve are characterized by the condition $dU/dI = 0$. For $E_{\rm act} > 4k_B T_a$, irrespective of the exponent α in Eq. (1), the temperature increase $\Delta T_{1,2} = T_{1,2} - T_a$ at the two turnover points becomes

$$\frac{\Delta T_{1,2}}{T_a} = \frac{E_{\rm act}}{2k_B T_a}\left(1 \mp \sqrt{1 - \frac{4k_B T_a}{E_{\rm act}}}\right) - 1. \quad (7)$$

The temperature rises at the turnover points depend only on the normalized activation energy $E_{\rm act}/(k_B T_a)$. Along the S-shaped current-voltage characteristics, two stable branches exist: an "ON" state with high conductivity and an "OFF" state with low conductivity, whereas the intermediate NDR region is unstable; see Fig. 1. This bistable behavior of the IV characteristic is related to thermal switching at the turnover points with $dI/dU \to \infty$,

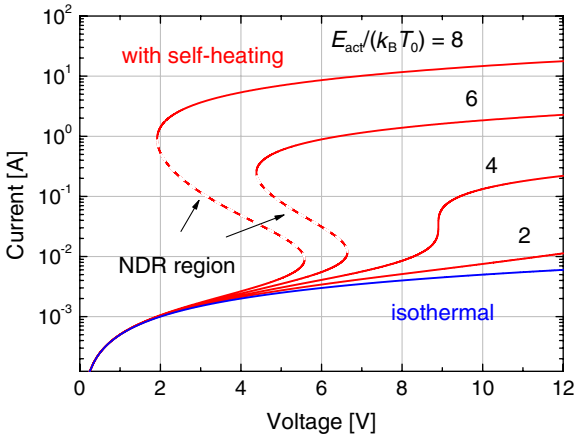

FIG. 1 (color online). Self-consistent current-voltage characteristics including self-heating according to Eqs. (4) and (5) (red), revealing that thermal switching can only occur above the critical value of the activation energy $E_{\rm act} > 4k_B T_a$. Unstable NDR regions are indicated by dashed lines. Thermal resistance $\Theta_{\rm th} = 1000$ K/W. Blue line: isothermal current-voltage relation (1) with $\alpha = 1$ at ambient temperature $T_a = T_0 = 293$ K.

involving a hysteresis loop [20], where the switching between the low conductivity OFF and the high conductivity ON branches occurs.

The IV characteristics of the intrinsic device show that the pure S-shaped NDR (S-NDR) behavior described by Eqs. (4) and (5) together with a load resistance $R_{\rm L}$ in series can again be parametrized by an increased temperature $T \geq T_a$. The resulting characteristic $(U_{\rm tot}(T),\ I(T))$ involves a modified total voltage along the load line $U_{\rm tot}(T) = U(T) + R_{\rm L} I(T)$, where $U(T)$ and $I(T)$ are defined in Eqs. (4) and (5), respectively. Turnover points are characterized by $dU/dI + R_{\rm L} = 0$, corresponding to a tangency condition for the intersection points between the load line and the IV characteristic of the S-NDR element itself [13,20]. For sufficiently small load resistance, namely, for $-\min(dU/dI) > R_{\rm L}$, the hysteresis effect is preserved, so that thermal switching between the ON and OFF states remains possible. The impact of a load resistance on the IV characteristic of the circuit calculated for a device with linear isothermal IV relation ($\alpha = 1$, $U_{\rm ref}/I_{\rm ref} = 2000\ \Omega$) is shown in Fig. 2. By an appropriate choice of load resistance, it may be possible to reduce the dissipated power in the ON state to a value that does not destroy the device by thermal runaway, but still preserves thermal switching. A further increase of the load resistance suppresses thermal switching ($R_{\rm L} > 55\ \Omega$ in Fig. 2), leading to a stabilization of the NDR region present in the intrinsic device [20]. For large voltages, the behavior is asymptotically dominated by the load resistance; see Fig. 2.

A suitable test structure requires an organic material with a sufficiently large conductivity, an activation energy $E_{\rm act} > 4k_B T_a$, thermal stability up to rather high temperatures, and negligible influence of injection barriers. Moreover, the thermal resistance $\Theta_{\rm th}$ must lead to a

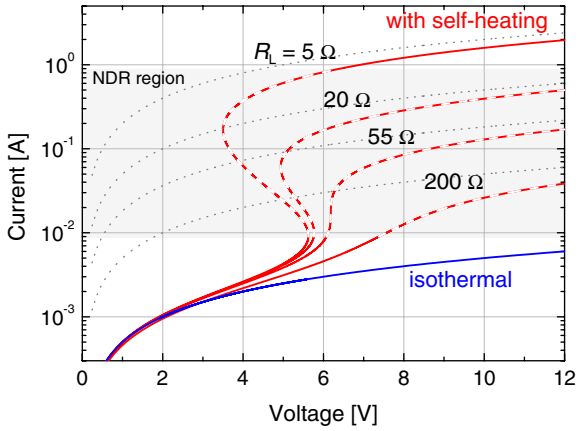

FIG. 2 (color online). Calculated current-voltage characteristics of an electrical circuit consisting of a device including self-heating together with a load resistance R_L in series (red), for $E_{act} = 8k_BT_a$, a thermal resistance $\Theta_{th} = 1000$ K/W, and different values of the load. The dashed parts indicate the NDR region of the intrinsic device as shown in Fig. 1. Blue line: isothermal current-voltage relation (1) with $\alpha = 1$ at constant temperature T_a. Black dotted lines indicate load resistance only.

substantial increase of the device temperature at moderate voltages.

All these requirements are perfectly met by nin-C_{60} crossbar structures grown on glass substrates, employing 20 nm thick n-doped C_{60} (n-C_{60}) layers adjacent to the metallic contacts, an intrinsic layer (i-C_{60}) with a thickness of 300 nm in between, and a relatively small active area of about 0.06 mm^2. Hence, a radius to thickness ratio of 10^3:1 characterizes the electronically conducting part of the sample. In Ref. [21], we investigated the temperature distribution in these devices by comparing measurements and simulations. Temperature stability up to 230 °C, an Ohmic behavior up to 0.1 V, and symmetric injection have been demonstrated for different thicknesses of the intrinsic layer [21]; see also the Supplemental Material [22].

From conductivity measurements in the temperature range from 200 to 300 K, we have obtained an activation energy of $8.2k_BT_0$, $T_0 = 293$ K, sufficiently large to allow for thermal switching; compare in Fig. 3. In these measurements, the voltage is kept fixed at 1 V and measured with a time step of 2 ms to avoid self-heating (see Supplemental Material [22]). Please note that the activation energy is a feature of the whole device, comprising both doped and intrinsic C_{60} layers, with a value in the same range as that in recent studies of C_{60} OFETs covering 4 orders of magnitude in charge carrier densities [23].

Since thermal switching is accompanied by a large increase of the sample temperature, it was found convenient to reduce the ambient temperature to a value of $T_a = 221$ K by a Peltier cryostat. The resistance of electrodes and measurement setup is about 7 Ω [21] and is increased by an additional series resistance of 5 Ω.

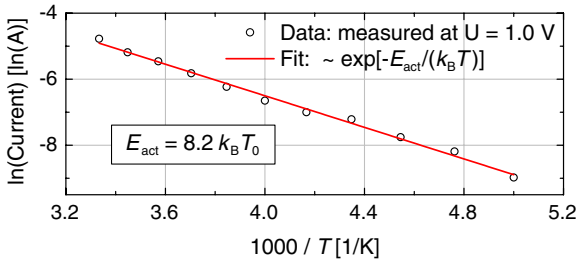

FIG. 3 (color online). Measurement of the current at $U = 1.0$ V over temperature, revealing an activation energy of $E_{act} = 8.2k_BT_0$. The possible influence of self-heating can be excluded by reducing the time per measurement point to 2 ms (see Supplemental Material [22]).

The current-voltage characteristics in Fig. 4 are measured in a voltage sweep from 1 to 3 V and back, with voltage steps of 5 mV held for time intervals of 0.15 s using a Keithley SMU 2400 device. At a voltage of 2.80 V, the circuit switches from the low conductivity OFF state to the high conductivity ON state. As long as we apply sufficiently large voltages, the system stays on the upper branch, but at 2.57 V it switches back to the OFF state, with a pronounced hysteresis between the two switching voltages. The thermal character of the switching becomes obvious when compared to a measurement with short voltage pulses (Keithley 2635A, pulse width, 200 μs; repetition time, 200 ms). In this measurement, the curve can simply be described by a power law with an exponent $\alpha = 2.75$, $U_{ref} = 23$V, and $I_{ref} = 1$ A in Eq. (1), without any signature of an increase in sample temperature.

The theoretical approach outlined above can be used to assign the key parameters of our device. Applying Eqs. (4) and (5) together with a load resistance, we obtain the best agreement between measured and calculated

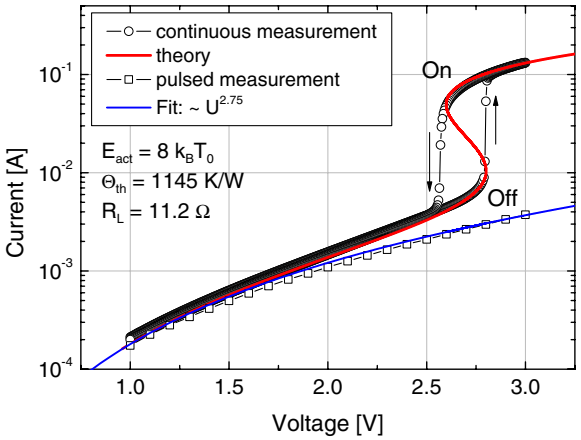

FIG. 4 (color online). Thermal switching measured during a voltage sweep upwards and downwards. For comparison, an isothermal current voltage characteristic is measured by applying short voltage pulses. The sample is cooled to $T_a = -52$ °C (221 K).

current-voltage characteristics when assuming an activation energy of $E_{act} = 8k_BT_0 = 10.6k_BT_a$, in good agreement with the value obtained for a fixed value of $U = 1$ V, a load resistance of $R_L = 11.2\ \Omega$, and a thermal resistance of $\Theta_{th} = 1145$ K/W; see Fig. 4. The thermal resistance is in the same range as the value of about 1000 K/W obtained by simulations of the heat flow [21].

Our fitting procedure demonstrates that the bistability is a natural consequence of the thermally activated conductivity in the organic electronic circuit. Residual deviations between theory and measurement along the ON state at a voltage about 2.6 V may be due to the simplifying assumption of homogeneous steady states. After switching back to the OFF state, the voltage sweep downwards reproduces the previous sweep upwards, indicating that the device has not been damaged by passing through the entire hysteresis loop. We can exclude the possible influence of a phase change in crystalline C_{60} at 251 K onto the thermal switching because such a phase change would decrease the conductivity by a small amount instead of increasing it by 1 order of magnitude, as observed [24,25]. Changes of charge carrier concentration due to impact ionization at high electric fields can be neglected since they cannot contribute significantly at voltages below 3 V [26] and, when present, they would also be observed in the measurement with short pulses. Consequently, the conductivity switching can be completely explained by purely thermal effects, revealing that nin-C_{60} devices constitute an interesting model system for further studies of thermally induced bistability.

The *S*-shaped *IV* curve of thermistors possesses a NDR region induced by self-heating. By two-wire measurements, we are not able to obtain the *IV* characteristic of the *S*-NDR element directly since a certain series resistance is already included within the device and measurement setup. In order to recover the pure *IV* curve of the organic *S*-NDR element itself, we have to subtract the voltage drop over the load resistance R_L from the measured voltage U_{tot} and obtain $U = U_{tot} - R_L I$. In Fig. 5, the measured current is plotted in dependence of the recalculated voltage using the resistance $R_L = 11.2\ \Omega$ as determined by the fit to theory. While switching into the ON state along the load line, the device exhibits a NDR, resulting in a strong reduction of resistance by a factor of more than 100. By using the analytical expression underlying the fit shown in Fig. 4, we can estimate the temperature at each point on the curve. As the highest temperature, we obtain 178 °C, still significantly below values of more than 200 °C obtained when stressing similar devices at even higher voltages [21].

In conclusion, for organic semiconductors we have demonstrated thermal switching and a pronounced hysteresis loop as a natural consequence of the bistability induced by an *S*-shaped *IV* characteristic. A significant impact of further phenomena such as phase changes, device degradation, or electronic effects such as avalanche generation can be excluded, making these easy-to-build C_{60}-crossbar structures an ideal model system for studies of thermal switching phenomena. Since all amorphous organic semiconductors show Arrhenius-like conductivity laws, our results have a significant impact on various types of organic devices, including OLEDs, OFETs, and high-power rectifying diodes. Even in cases where thermal switching is inhibited by a large series resistance, self-heating can lead to a negative differential resistance so that all organic devices with sufficiently large activation energies have to be understood as thermistors. In particular, the activation energy is an important material property in applications with considerable Joule heat. Symmetry-breaking perturbations increased by NDR can promote current filaments [18,27] or other spatial inhomogeneities [20]. Hence, multidimensional simulations are required for a deeper understanding of charge and heat transport.

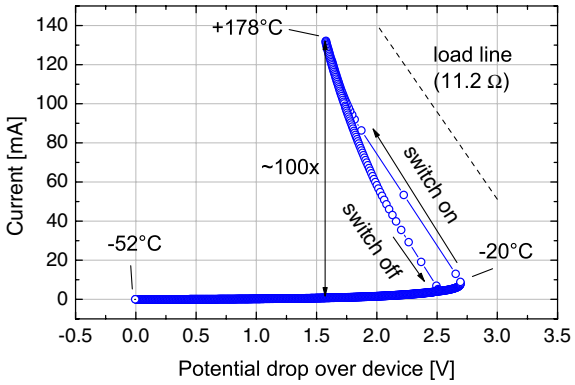

FIG. 5 (color online). Current-voltage characteristic of the organic *S*-NDR element recovered by $U = U_{tot} - R_L I$ with load resistance $R_L = 11.2\ \Omega$ from the measured data (U_{tot}, I) plotted in Fig. 4 showing the switching along the load line. The dashed line is a guide to the eye for the load line. The highest temperature achieved is about 178 °C, or 230 K above the ambient temperature in the Peltier cooler.

Especially large area OLEDs can be understood as a parallel thermistor array: because of an inhomogeneous current flow through the device—unavoidable in the case of locally contacted indium-tin-oxide—the areas with high local current would enhance the current flow by the self-heating effect and might lead to inhomogeneous light emission or degradation effects. In particular, we observed *S*-NDR in OLED devices, enhancing the spatial inhomogeneity of power dissipation and light emission in OLED lighting panels [28].

This work received funding from the Deutsche Forschungsgemeinschaft (DFG) within the Collaborative Research Center CRC 787 "Semiconductor Nanophotonics" (Th. K.), the DFG Research Center MATHEON under Project No. D22 (A. G.), and the European Community's Seventh Framework Programme under Grant Agreement No. FP7-267995 (NUDEV) (A. F.).

*Corresponding author.
axel.fischer@iapp.de
†Corresponding author.
thomas.koprucki@wias-berlin.de

[1] J. Park, J. Lee, and Y.-Y. Noh, Org. Electron. **13**, 184 (2012).
[2] C. Gärditz, A. Winnacker, F. Schindler, and R. Paetzold, Appl. Phys. Lett. **90**, 103506 (2007).
[3] X. Zhou, J. He, L. S. Liao, M. Lu, X. M. Ding, X. Y. Hou, X. M. Zhang, X. Q. He, and S. T. Lee, Adv. Mater. **12**, 265 (2000).
[4] S. Steudel, K. Myny, V. Arkhipov, C. Deibel, S. De Vusser, J. Genoe, and P. Heremans, Nat. Mater. **4**, 597 (2005).
[5] W. F. Pasveer, J. Cottaar, C. Tanase, R. Coehoorn, P. A. Bobbert, P. W. M. Blom, D. M. de Leeuw, and M. A. J. Michels, Phys. Rev. Lett. **94**, 206601 (2005).
[6] S. L. M. van Mensfoort, S. I. E. Vulto, R. A. J. Janssen, and R. Coehoorn, Phys. Rev. B **78**, 085208 (2008).
[7] H. Bässler and A. Köhler, in *Unimolecular and Supramolecular Electronics I*, Topics in Current Chemistry, Vol. 312, edited by R. M. Metzger (Springer, Berlin/Heidelberg, 2012), pp. 1–65.
[8] K. W. Wagner, Trans. Am. Inst. Electr. Eng. **XLI**, 288 (1922).
[9] L. Inge, N. Semenoff, and A. Walther, Z. Phys. A **32**, 273 (1925).
[10] N. Semenoff, Z. Phys. A **48**, 571 (1928).
[11] J. A. Becker, C. Green, and G. L. Pearson, Trans. Am. Inst. Electr. Eng. **65**, 711 (1946).
[12] R. E. Burgess, Proc. Phys. Soc. London Sect. B **68**, 908 (1955).
[13] C. Popescu, Solid State Electron. **13**, 441 (1970).
[14] N. Croitoru and C. Popescu, Phys. Status Solidi (a) **3**, 1047 (1970).
[15] N. Klein, Thin Solid Films **7**, 149 (1971).
[16] C. Berglund and N. Klein, Proc. IEEE **59**, 1099 (1971).
[17] W. Haubenreisser, W. Löser, C. Mattheck, K.-H. Möckel, and E. Steinbeiss, Phys. Status Solidi (a) **22**, 427 (1974).
[18] M. Shaw, V. Mitin, E. Schöll, and H. Grubin, *The Physics of Instabilities in Solid State Electron Devices* (Plenum Press, New York, 1992).
[19] M. Schober, M. Anderson, M. Thomschke, J. Widmer, M. Furno, R. Scholz, B. Lüssem, and K. Leo, Phys. Rev. B **84**, 165326 (2011).
[20] E. Schöll, *Nonequilibrium Phase Transitions in Semiconductors* (Springer, Berlin/Heidelberg, 1987), Chap. 6.2.
[21] A. Fischer, P. Pahner, B. Lüssem, K. Leo, R. Scholz, T. Koprucki, J. Fuhrmann, K. Gärtner, and A. Glitzky, Org. Electron. **13**, 2461 (2012).
[22] See Supplemental Material at http://link.aps.org/supplemental/10.1103/PhysRevLett.110.126601 for discussion about phase change in C_{60}, activation energy, and origin of the thermal switching in the device.
[23] I. I. Fishchuk, A. K. Kadashchuk, J. Genoe, M. Ullah, H. Sitter, T. B. Singh, N. S. Sariciftci, and H. Bässler, Phys. Rev. B **81**, 045202 (2010).
[24] H. Peimo, X. Yabo, Z. Xuejia, Z. Xinbin, and L. Wenzhou, J. Phys. Condens. Matter **5**, 7013 (1993).
[25] E. A. Katz, D. Faiman, B. Mishori, Y. Shapira, A. Isakina, and M. A. Strzhemechny, J. Appl. Phys. **94**, 7173 (2003).
[26] G. Wachutka, IEEE Trans. Electron Devices **38**, 1516 (1991).
[27] J. J. M. van der Holst, M. A. Uijttewaal, B. Ramachandhran, R. Coehoorn, P. A. Bobbert, G. A. de Wijs, and R. A. de Groot, Phys. Rev. B **79**, 085203 (2009).
[28] A. Fischer, R. Scholz, B. Lüssem, K. Leo, T. Koprucki, K. Gärtner, and A. Glitzky, unpublished results.